Title:

Network-Level Changes in the Brain Underlie Fear Memory Strength

Running title:

Brain Networks of Mild and Strong Fear

Authors:

Josue Haubrich[1,2] & Karim Nader[1]

1 Department of Psychology, McGill University, Canada

2 Department of Neurophysiology, Ruhr-University Bochum, Germany

Corresponding author: Josue Haubrich, PhD.

Dept. of Neurophysiology. Medical Faculty. Ruhr-University Bochum. Universitätsstraße 150, MA 4/150. 44780 Bochum, Germany.

Phone: +49 015 255 849095

E-mail: josue.haubrich@rub.de / josuehaubrich@hotmail.com

Abstract

The strength of a fear memory significantly influences whether it drives adaptive or maladaptive behavior in the future. Yet, how mild and strong fear memories differ in underlying biology is not well understood. We hypothesized that this distinction may not be exclusively the result of changes within specific brain regions, but rather the outcome of collective changes in connectivity across multiple regions within the neural network. To test this, rats were fear conditioned in protocols of varying intensities to generate mild or strong memories. Neuronal activation driven by recall was measured using c-fos immunohistochemistry in 12 brain regions implicated in fear learning and memory. The interregional coordinated brain activity was computed and graph-based functional networks were generated to compare how mild and strong fear memories differ at the systems level. Our results show that mild fear recall is supported by a well-connected brain network with small-world properties in which the amygdala is well-positioned to be modulated by other regions. In contrast, this connectivity is disrupted in strong fear memories and the amygdala is isolated from other regions. These findings indicate that the neural systems underlying mild and strong fear memories differ, with implications for understanding and treating disorders of fear dysregulation.

INTRODUCTION

Whether a fear memory leads to adaptive or maladaptive behavior can be determined by the intensity of the initial aversive experience. A deeper understanding of fear memory requires identifying changes in the neural mechanisms engaged by fear memories of varying levels of aversiveness. Research on rodent fear conditioning has been mostly conducted in mild protocols and comparisons with strong protocols are scarce. While this approach advances our understanding of normal fear memories, it leaves open questions about specific mechanisms in disorders of fear dysregulation, such as post-traumatic stress disorder (PTSD) [1].

Normal fear memories are critical to survival. These memories trigger appropriate responses that are cue-specific and can be attenuated by extinction [2–4]. These adaptive representations are flexible and their content may be updated upon recall through reconsolidation [5–8]. Importantly, these fear memories can be disrupted by pharmacological interventions targeting their reconsolidation [9–12], offering a wealth of clinical possibilities [13]. However, severe aversive events can lead to the formation of strong, maladaptive fear memories that trigger disproportionate and generalized fear responses [14–16] and tend to be resistant to extinction [17] and to undergo reconsolidation [18–21].

The formation and expression of fear memories are believed to rely on the coordinated activity of a network of brain structures. The amygdala is an integral structure in all aspects of fear memory formation and expression [22, 23]. Subsequent to severe fear learning, it has been shown that changes take place in the composition of glutamate receptors in the amygdala that are linked to maladaptive memories [19, 21, 24, 25]. In the case of contextual fear memories, the involvement of the hippocampus also becomes critical given its role in the processing of context-related information [26–28]. Other regions, such as the retrosplenial, infralimbic, prelimbic, and cingulate cortices, and the reuniens and paraventricular nuclei of the thalamus, also play important roles in modulating fear memories [4, 29–32]. Importantly, the action of stress hormones and the locus coeruleus-noradrenaline system plays a key role in the formation of maladaptive-like fear memories [25, 33, 34]. It is not clear how the coordinated activity

between these regions changes with the severity of fear memories but basic and clinical findings suggest it may be dysregulated [35].

The distinctions between adaptive and maladaptive memories may not be solely attributed to changes within isolated structures or altered connectivity between pairs of structures, but rather to collective changes across multiple structures within the neural network. Combining the quantification of immediate-early genes expression linked to neural activation such as c-fos [36] and network-based graph analysis [37–39], it is possible to reveal the brain functional connectivity during active cognitive experiences, such as memory recall [40–43]. In network models of neural systems, brain regions are represented as nodes, and functional connections between nodes are represented as edges. Multiple measures can be computed to inform the relationship between nodes and the global characteristics of the network, which can elucidate changes in information processing across different conditions.

In this study, we aimed to shed light on the system mechanisms underlying the recall of mild and strong fear memories. First, we established the behavioral differences triggered by fear conditioning protocols of varying intensities. We then employed c-fos immunohistochemistry to measure brain activation in 12 brain areas critical for fear learning and memory during the recall of mild and strong fear. Subsequently, the interregional coordinated brain activity was computed and functional networks were generated. Our findings indicate that the system mechanisms of fear memories vary based on their intensity, as a mild fear recall is supported by a well-connected network while the recall of strong fear is associated with disruptions in network connectivity.

MATHERIALS AND METHODS

Subjects

Male Sprague Dawley rats (275–300 g at arrival; Charles River, Quebec, Canada) were housed in pairs in plastic cages in a temperature-controlled environment (21–23°C) with ad libitum access to food and water and maintained on a 12 hr light/dark cycle (lights on at 7:00 A.M.). All experiments were conducted during the light phase. In all experiments, animals were randomly assigned to each behavioral condition. Sample size estimates were determined based on effect sizes observed in previous reports using similar assays [21, 25, 44] resulting in statistical power estimates between 70% and 90%. Each rat was handled for at least 5 days before the behavioral procedures. All procedures were approved by McGill's Animal Care Committee (Animal Use Protocol #2000–4512) and complied with the Canadian Council on Animal Care guidelines.

Drugs

Anisomycin (150 mg/kg, i.p.; Sigma-Aldrich) was dissolved in equimolar HCl and sterile saline and had its pH adjusted to 7.5.

Contextual fear conditioning and behavioral testing

The training session, which lasted 12 minutes in all groups, took place in transparent Plexiglas conditioning boxes enclosed in soundproofed chambers (30 × 25 × 30 cm; Coulbourn Instruments) with a fan on as background noise. Animals assigned to the 2-shocks group (2S) received 2 x 1s x 1.0 mA foot shocks at the sixth and seventh minutes, while animals in the 10-shocks group (10S) received foot shocks every minute from the second to the eleventh minute. A stainless-steel grid floor provided the shocks.

The recall and extinction sessions were conducted in the same context as the fear conditioning session, with recall lasting 4 minutes and extinction lasting 30 minutes. The generalization test, which also lasted 4 minutes, was conducted in different conditioning boxes with white-striped front and back walls and rounded white plastic walls on the sides, as well as a white plastic floor. Different sessions were always conducted 24 hours apart. Behavior was recorded by digital cameras and memory was evaluated by a

blind experimenter measuring the time spent freezing, using Freeze View software (Actimetrics). In the analysis of fear expression during the training session, due to technical issues, we could only assess six out of eight animals in the 2S group. Freezing was defined as immobilization except for respiration. The generalization index was calculated as Freezing in Test B / (Freezing in Test A + Freezing in Test B).

The open field test lasted 5 minutes and was conducted in a 1 m^2 grey Pexiglass arena. Behavior was recorded by digital cameras and analyzed with the software EthoVision (Noldus, The Netherlands).

Immunohistochemistry

After 90 minutes of testing, rats were anesthetized and perfused with buffered saline followed by 4% paraformaldehyde (PFA). The brains were then collected, fixed in 4% PFA overnight, transferred to a 30% sucrose solution, and stored at 4°C until cryo-sectioning at 50 µm thickness. To measure c-fos expression, coronal brain slices were incubated in a blocking solution at room temperature for 1 hour (3% NGS, 0.3% Triton X-100) and then for 20 hrs with anti-c-fos primary rabbit antibody (1:500, 226.003; Synaptic Systems, Göttingen, Germany). Sections were washed and incubated with anti-rabbit Alexa-488 secondary antibody (1:500, Jackson Immunoresearch, West Grove, PA) for 2 hr at room temperature. The sections were washed again and mounted on slides and immediately coverslipped with Fluoromount-G with DAPI (Thermo Fisher). Images were examined under fluorescence microscopy (Leica DM 5000 B) and c-fos -positive cells were counted bilaterally from at least two slices for each animal with ImageJ.

Statistics and networks generation

To analyze the results of the behavioral tests and c-fos expression, we used two-tailed independent-samples t-test, one-way, two-way, or two-way repeated measures ANOVA

for data analysis. Tukey's p*ost hoc* tests were further used to identify the specific differences that contributed to significant interactions. Type-one error rate was set at 0.05.

For the analysis of functional connectivity, Pearson correlation coefficients were computed for all pairwise correlations of c-fos expression levels across the 12 targeted regions of interest within each group. To compare mean r values between groups we used the Kruskal-Wallis test followed by post hoc Mann-Whitney tests.

The functional networks were generated by considering only the strongest correlations, as determined by a threshold of Pearson's r values that were higher than the mean plus the standard deviation of all correlations. This thresholding approach was used to provide a cut-off based on the data's inherent distribution, therefore retaining the top edges according to the data variance. The networks were generated and centrality measures were computed using the R package igraph (igraph.org/r) and custom R code (github.com/johaubrich). The nodes in the network represent brain regions, and the correlations retained after thresholding were considered as edges, with the r value being assigned as the edge's weight. Degree denotes the total number of edges connected to a particular node. Betweenness represents the number of times a node appears on the shortest paths between two other nodes. The shortest path is the length of the path connecting two nodes with the lowest number of edges. The nodal efficiency of each node was calculated as the average inverse of the shortest path length to all other nodes in the network. For the nodal efficiency calculation, the average path distance considered the weight of the edges (i.e. 1/r value). The global efficiency denoted the average nodal efficiency of all nodes within a network. Comparisons of degree, betweenness, and global efficiency were conducted using Kruskal-Wallis tests followed by Mann-Whitney tests. For the small-world analysis, we generated 1000 random networks for each group using the Watts-Strogatz small-world model [45]. To ensure that the random networks had a similar density and could provide a suitable comparison for global efficiency, these networks were generated enforcing a similar clustering coefficient [46] to their respective memory network (calculated with 1000 iterations per network). The global efficiency of the networks for the NS, 2S, and 10S

groups was compared to their respective random networks by calculating the 95% confidence interval of the difference between means.

All statistical analysis and plots were generated using RStudio® (R version 4.2.2, RStudio version 2022.12.0).

RESULTS

1. The effect of varying fear conditioning intensity on behavioral responses

In order to investigate fear memories of different intensities, animals underwent contextual fear conditioning with either two (2S) or ten foot shocks (10S). A control group, in which no shock was administered, was included to provide a baseline behavior (NS). After training, a series of behavioral tests were conducted to determine the characteristics of the resulting memory. One day after training, we assessed the intensity of fear responses triggered by the conditioned context (Test A), and on the following day, fear generalization in a novel context (Test B). In addition, changes in exploratory behavior were assessed in an open-field exploration test conducted three days after training.

During training (Figure 1A, middle), repeated-measures ANOVA indicated a significant effect of group ($F_{2,19} = 255.2$, $p < 0.001$), bin ($F_{11,209} = 130.4$, $p < 0.001$), and group x bin interaction ($F_{22,209} = 43.77$, $p < 0.001$). Tukey's post hoc revealed that in the 2S group, freezing levels during the concluding four minutes surpassed all previous time bins ($p < 0.001$). In the 10S group, the first three minutes exhibited lower freezing relative to all other bins ($p < 0.05$), and the last 6 minutes did not differ from each other ($p > 0.05$). This indicates that freezing behavior increased after shock presentations and showed no decline towards the session's end.

The results of Test A and Test B showed that freezing behavior increased as a function of the training intensity (Figure 1A, bottom left). Repeated-measures ANOVA indicated a significant effect of group ($F_{2,21} = 166$, $p < 0.001$) and group x session interaction ($F_{2,21} = 12.86$, $p < 0.001$). Tukey's post hoc indicated that in context A all groups differed from each other ($p < 0.001$) with the 10S displaying the higher freezing levels. During the test in context B there was no difference between NS and 2S groups ($p = 0.31$) while the 10S group was higher than all others ($p < 0.001$). To compare fear generalization between animals trained with 2 shocks and 10 shocks, a discrimination index was computed and compared, and a Student's t-test revealed that there was a significant difference between groups (Figure 1.A, bottom center; $t(14) = -2.3$, $p = 0.037$).

In the open field test conducted one day after test 2 (Figure 1A, bottom right), there were no group differences in the time spent in corners ($F_{2,24} = 0.987$, $p = 0.4$) and total distance moved ($F_{2,24} = 1.52$, $p = 0.1$). There were also no differences in the time spent in the center ($F_{2,24} = 0.302$, $p = 0.7$), number of quadrant crossings ($F_{2,24} = 1.2$, $p = 0.3$), number of crossings on the center ($F_{2,24} = 0.301$, $p = 0.7$), average speed ($F_{2,24} = 1.56$, $p = 0.2$) - data not shown. Thus, suggesting that differences in freezing performance are due to alterations in memory expression and not in motor abilities.

We then evaluated the effect of training intensity on fear extinction (Figure 1B). Repeated-measures ANOVA indicated a significant effect between groups ($F_{1,14} = 6.67$, $p = 0.02$), bin ($F_{6,84} = 14.4$, $p < 0.001$), and no group x bin interaction ($F_{6,84} = 1.7$, $p = 0.12$). Tukey's post hoc revealed that the 2S group displayed extinction retention since there was no difference between the last extinction bin and the test session the next day ($p = 0.9$), but in the 10S group there was a significant increase in freezing ($p = 0.003$) that returned to the levels found in the first bin ($p = 0.72$). Furthermore, in the 2S group, freezing during test remained consistent with the levels observed in the final extinction bin ($p = 0.61$) and was lower than the levels in the initial extinction bin ($p < 0.001$), indicating no spontaneous recovery. Conversely, in the 10S group, freezing levels increased from the final extinction bin to the test ($p = 0.003$), reaching levels comparable to those observed in the first extinction bin ($p = 0.19$), indicating complete spontaneous recovery.

Next, we investigated the effect of training intensity on the ability of memory to change through reconsolidation. One day after the initial training, memory was reactivated by a 5-minute re-exposure to the training context, followed immediately by the injection of the protein synthesis inhibitor anisomycin. To verify if reconsolidation was disrupted by the treatment, animals were re-exposed to the context the next day (Figure 1C). Repeated-measures ANOVA indicated a significant effect between groups ($F_{1,28} = 97.9$, $p < 0.001$) and a group x session x treatment interaction ($F_{1,28} = 8.72$, $p = 0.006$). Tukey's post hoc revealed that in the 2S group, post-reactivation anisomycin lead to a decrease in freezing during the test ($p < 0.001$), while the freezing levels of vehicle-treated animals remained constant ($p = 0.9$). In contrast, freezing in the 10S group did not change

across sessions in both animals that received vehicle ($p = 0.36$) and anisomycin ($p = 0.25$). This suggests that memories formed with the stronger training protocol (10S group) are resistant to change upon recall

These data demonstrate that memories formed with 2- and 10-shock protocols exhibit significant differences at the behavioral level. Secondly, they show that 10-shock training creates maladaptive memories that trigger intense and generalized fear responses, are resistant to suppression by extinction, and are unable to flexibly change through reconsolidation.

2. Commonalities and differences in brain activation induced by recall of mild and strong fear memories

To investigate the neural mechanisms underlying the formation of mild and strong fear memories, we trained a new cohort of animals using the same contextual fear conditioning (CFC) protocol as described in the previous experiments. We then performed IHC to count c-fos expressing cells and measure brain activation during memory recall in 12 brain regions implicated with fear memory processes (Figure 2). Based on previous literature, we examined the following regions: the retrosplenial cortex (RSC), the infralimbic cortex (IL), the cingulate cortex area 1 and area 2 (Cg1 and Cg2), the dentate gyrus (DG) and the CA3 and CA1 hippocampal fields, the basolateral and central nuclei of the amygdala (BLA and CeA), and the paraventricular and the reuniens nuclei of the thalamus (PV and Re).

Similar to our first set of experiments, there was a significant difference in freezing expression between groups during test (one-way ANOVA: $F_{2,21} = 118.4$, $p<0.0001$) and freezing expression increased according to the training intensity (Tukey's *post hoc* test: NS x 2S: $p < 0.0001$; NS x 10S: $p < 0.0001$; 2S x 10S: $p = 0.033$).

In the c-fos analysis, the data were normalized to the average of the NS group (Figure 2.C). ANOVA indicated a significant difference between groups in the following brain regions: RSC ($F_{2,21} = 6.39$, $p = 0.007$), Re ($F_{2,21} = 5.22$, $p = 0.014$), IL ($F_{2,21} = 4.18$, $p = 0.03$), BLA ($F_{2,21} = 14.9$, $p < 0.0001$), CeA ($F_{2,21} = 22.8$, $p < 0.0001$), and PV

($F_{2,21}$ = 12.9, p = 0.0002). Tukey's *post hoc* test was then performed to reveal pairwise differences between groups within each structure. In the RSC and in the Re, c-fos levels were higher than NS controls only in the 2S group (p = 0.005 and p = 0.01, respectively), while in the IL c-fos was reduced in the 10S group in comparison with the 2S group (p = 0.03). Both 2S and 10S groups displayed higher c-fos levels than NS controls in the BLA (NS x 2S: p = 0.003; NS x 10S: p < 0.0001), CeA (NS x 2S: p = 0.042; NS x 10S: p = 0.001), and PV (NS x 2S: p = 0.010 NS x 10S: p = 0.0001). In addition, there was an increase in c-fos in the 10S group in comparison with the 2S group (p = 0.0014). These results show that the retrieval of mild and strong fear memories triggers different patterns of brain activation across different brain regions.

3. Coordinated interregional brain activity is decreased during strong fear memory recall

When the activity of a pair of brain regions varies together, it can be inferred that these regions are functionally coupled[43]. To further understand the mechanisms underlying the recall of memories with varying levels of aversiveness, we investigated if there were changes in the coordinated activity between brain regions. Therefore, we assessed the synchrony in neuronal activation across brain regions by computing the Pearson correlations between all pairs of brain regions within each group (Figure 3.A).

We first compare the distribution of r values between groups (Figure 3.B) using Kruskal-Wallis followed by Mann-Whitney tests. This revealed a significant difference between groups regarding r values (H = 0.118, df = 2, p < 0.001), such that the r values of the 2S group were larger than those of the NS (p < 0.001) and 10S (p < 0.001) groups, which did not differ from one another (p = 0.13).

Next, we conducted the same analysis but compared the r values in collections of brain regions (Figure 3.C): the amygdala (Amyg: CeA and BLA) hippocampal fields (HPC: DG, CA3, and CA1), the prefrontal cortex (PFC: PL, IL, Cg1, and Cg2), and the remaining structures that were quantified (Other: RSC, PV, and Re). There was a significant difference between groups in the amygdala (H = 0.157, df = 2, p = 0.003),

hippocampus ($H = 0.05$, $df = 2$, $p = 0.03$), prefrontal cortex ($H = 0.166$, $df = 2$, $p < 0.001$) and in the remaining structures ($H = 0.08$, $df = 2$, $p = 0.009$). Subsequent Mann-Whitney tests revealed that, in the 2S group, the r values were significantly larger than the NS or 10S groups in all structures ($p < 0.05$) except in the hippocampus, where it did not differ from 10S rats ($p = 0.14$). In all regions, NS and 10S groups did not differ ($p > 0.05$).

The results indicate that the level of coordinated activity between brain regions, as indicated by r values, changes during the recall of memories with varying levels of aversiveness. Compared to the re-exposure to a neutral context (NS group), the recall of a mild fear memory (2S group) was found to be associated with an increase in the level of coordinated activity across brain regions. However, this increase in coordinated activity was not observed during the recall of a severe fear memory (10S group).

4. Network-Level Changes in the Brain Underlie the Intensity of Fear Memories.

Having established that the levels of coordinated activity during recall vary according to the intensity of the memory, we employed graph theory to construct functional networks and gain a deeper understanding of the interactions between brain systems in each condition.

The networks were constructed such that each node represents a brain region, and edges connecting the nodes are weighted according to the respective correlation coefficients (Figure 4.A). To generate functional networks, thresholding was applied to retain only the edges with the highest weights, which indicate the strongest coordinated activity and the most essential functional connections. This was accomplished by excluding edges with r values lower than the average plus one standard deviation of all networks (Figure 4.B; $r < 0.61$).

To measure the relevance of individual nodes within the networks and to gather insight into how the information flows within the networks, the degree centrality, betweenness centrality, and nodal efficiency were computed. The nodes were ranked according to each metric to reveal their relative importance in the respective network. The degree centrality measures the number of connections each node in the network has to other

nodes (Figure 4.C). The betweenness-centrality measures the instances in which a node acts as a bridge along the shortest path between two other nodes (Figure 4.D). The nodal efficiency measures the inverse of the average shortest path length between a node and all other nodes in the network and reflects its ability to exchange information with other nodes, whereas the global efficiency reflects how well the network communicates as a whole and is computed as the average nodal efficiency (Figure 4.E).

In the 2S network, the CeA and the BLA were among the highest-ranked nodes across measurements, indicating a central and well-connected position in the network. In contrast, the amygdala nuclei ranked low in the other groups. In the NS group, this is consistent with the lack of conditioned fear observed in these animals. In the 10S group, however, where conditioned fear was highly expressed during recall, this lower ranking suggests a reduction in the functional interactions between the amygdala and the other brain regions. Therefore, the brain-wide functional integration of the CeA and BLA observed in the mild fear memory network seems to be reduced in the severe fear memory network.

To gain a better understanding of how each network differed regarding their connectivity patterns, centrality measures were compared using Kruskal-Wallis followed by Mann-Whitney tests. When analyzing degree (Figure 4.C, right), it was found a significant difference between groups ($H = 0.226$, $df = 2$, $p = 0.009$), with the 2S network displaying higher degree values than NS and 10S ($p < 0.05$), which did not differ from each other ($p = 0.81$). Regarding betweenness (Figure 4.D, right), there was a significant overall group difference ($H = 0.272$, $df = 2$, $p = 0.005$) and the mild memory network scored higher than the strong ($p = 0.009$) but not than the NS network ($p = 0.06$), and the NS and 10S networks did not differ ($p = 0.25$). The values of global efficiency also differed among the memory networks (Figure 4.E, right; $H = 0.605$, $df = 2$, $p < 0.001$). The 2S network displayed higher values than NS and 10S networks ($p < 0.001$), which did not differ from each other ($p = 0.32$).

A feature of many complex networks, including anatomical and functional brain networks, is a small-world organization, which is characterized by a balance of high

local clustering but a small number of steps separating each node[38]. This balance enables rapid specialized local processing and efficient global communication, resulting in a robust and efficient network structure. To determine whether the memory networks generated in this study display global efficiency comparable to that of small-world networks, random networks were generated using the Watts-Strogatz small-world model [45]. The global efficiencies of the memory and random small-world networks were then compared through the calculation of the confidence interval for the difference between means (Figure 4.E, right). The 2S memory network matched the global efficiency of its respective random networks (mean difference = 0.012, 95% CI [-0.031, 0.056]). In contrast, the global efficiency of the memory networks was lower than those of the respective random networks in the case of the NS group (mean difference = 0.236, 95% CI [0.161, 0.309]) and of the 10S group (mean difference = 0.288, 95% CI [0.284, 0.327]).

These results demonstrate that, among the brain structures measured here, the level of aversive intensity of memory has a critical impact on functional connectivity during recall. In comparison to the neutral and severe fear memory networks, the mild fear memory network displayed higher functional connections between brain regions (degree), more nodes connecting different parts of the network (betweenness), and higher efficiency in global information flow that was consistent with that of small-world networks (global efficiency). Overall, this suggests that during mild fear memory recall, fear expression driven by the amygdala is modulated by a large, integrated interregional system, but in strong fear memories this modulation is disrupted.

This visualization of functional networks shows a closely connected network for the mild memory group, in contrast to the fragmented networks observed for the neutral and strong fear memory groups (Figure 4.F). Clusters in the networks were identified using a leading eigenvector method [47]. It revealed that in the mild memory network, there is a central cluster composed of the amygdala, Re, PV, and PL. A second cluster included the hippocampus, the IL, and RSC, and a third cluster comprised the cingulate cortex. This suggests that the amygdala is well positioned for interregional communication, potentially allowing for modulatory control of fear expression. This is not the case in the

strong memory network where the BLA and CeA are close to each other but isolated from other regions, resulting in less modulatory control of fear.

DISCUSSION

The present study investigated how functional connectivity during fear memory recall varies depending on fear memory intensity. Utilizing mild and strong fear protocols, we were able to generate memories that exhibit remarkable differences in their behavioral and neuronal signatures. Specifically, we found that mild memories triggered moderate and precise behavioral responses that were susceptible to extinction and reconsolidation, while strong memories triggered robust and generalized responses and were resistant to both extinction and reconsolidation. When comparing the brain activity across 12 regions implicated in fear memory, we found that recall resulted in changes in overall activity in only a subset of these regions. However, when we examined coordinated activity patterns, we discovered striking differences in the functional networks that underly mild and strong fear memory recall. Mild memories displayed a well-connected network with the amygdala, which was well-positioned to interact with and be influenced by several regions. However, such connectivity was absent in the strong fear memory network, which may underlie the observed high and generalized fear responses that are resistant to attenuation. These findings suggest that abnormal functional connectivity may be a core factor in maladaptive, severe fear memories.

To study brain differences between mild and strong fear memories, we used conditioning protocols of different intensities that generated fear memories remarkably different at the behavioral level. Conditioning with 2 shocks resulted in a fear memory eliciting mild and discriminative fear responses, which could be attenuated by extinction, and its recall triggered reconsolidation. In contrast, a 10-foot shock training generated a strong fear memory that can be seen as maladaptive - it elicited high and generalized fear expression which was resistant to undergo both extinction and reconsolidation. Importantly, our control animals were exposed to the conditioning chamber for an equivalent duration without being subjected to shocks, thus encoding and recalling a non-fearful contextual memory (Figure 1). The recall of these distinct memories resulted in differential brain activation in some structures. In line with the role of the amygdala [48–51] and paraventricular nucleus [52, 53] in fear expression, we observed that c-fos counts in these structures increased as a function of the strength of the fear memory.

Conversely, in the infralimbic cortex, c-fos expression was decreased in the 10S group, which is in line with its established role in safety learning and fear suppression [54, 55]). Adding to the known involvement of the RSC [56, 57] and the Re [58–60] in modulating fear memory formation and expression, our results revealed neural activity in these structures was increased during mild memory recall, but not during strong memory recall, when compared to unshocked controls. Although the hippocampus [49, 50, 61–63], prelimbic [64–66], and cingulate cortex [67–69] are critical to contextual fear memory-related processes, we found no differences in their activation between groups, suggesting that the role of these structures in modulating the expression of fear of different intensities may not reflect in changes in overall activation levels.

The amygdala is a central hub for the processing of fear memory and fear expression during recall. It receives input from sensory areas and integrates this information with several other brain regions, such as the hippocampus and the prefrontal cortex, to generate adaptive fear responses. The projections to the amygdala from these regions modulate the intensity of fear responses, extinction learning, and the induction of reconsolidation. Consequently, the functional connectivity of the amygdala within a memory network plays a crucial role in determining the level of fear expression. Our initial assessment of mean coordinated activity supports this concept. We found that, in comparison with unconditioned controls, the overall correlation values of the amygdala with other brain regions increase during the recall of a mild fear memory, but not during the recall of a strong fear memory.

The functional networks analysis further evaluated the system-level interactions of different brain regions during the recall of mild and severe fear memories. Centrality measures were computed to assess the number of functional connections, hub nodes, and information flow throughout the network. These measures were increased during the recall of mild fear memories compared to untrained controls, and such an increase was not observed during the recall of strong fear memories. Moreover, only the mild fear memory network displayed a small-world organization, which allows for both specialized and efficient information processing in the network. These findings suggest that the expression of moderate and flexible fear memories involves an efficient,

integrated activation of specific brain regions, which is not present in the recall of strong fear memories.

Importantly, both the basolateral and the central amygdala ranked high across the centrality measures assessed. Of particular importance is the high nodal efficiency ranking of the amygdala, indicating it was a main central mediator of information flow throughout the network. Notably, the infralimbic cortex, a region known to suppress fear responses by sending inhibitory projections to the amygdala [70], displayed the highest betweenness centrality during mild memory recall. However, during the recall of severe fear memory, the amygdala displayed a considerably lower ranking across centrality measures, similar to what was observed in control unconditioned animals. These changes in the network-level integration of the amygdala are apparent in the model depicted in Figure 4.F. In the 2S graph, the amygdala is at the center of a fully connected network and the IL is a critical bridge connecting the amygdalar module to the one containing the hippocampus and the retrosplenial cortex. In contrast, in the 10S graph, the amygdala is disconnected from the other regions. This indicates that the differences observed behaviorally during severe fear memory recall – high and generalized freezing and resistance to attenuation– coincided with a disruption in the functional connectivity of the amygdala with other regions that are important for regulating fear. To further elucidate the underlying mechanisms of fear memory strength in vivo, understanding the specific roles of individual network elements in fear regulation becomes essential. Future research will be important to probe the causal interplay among distinct nodes and edges, both individually and in combination, in shaping diverse aspects of fear expression.

To generate mild and strong fear memories, we based our conditioning parameters on methods that have shown distinct behavioral outcomes in prior studies [19, 21, 71–73]. To ensure a focused comparative analysis, our conditioning protocols differed only in the number of foot shocks, and maintained consistent shock intensities and session durations. Yet, the number of shocks is not the only factors that can affect the strength of fear memories [74]. Other conditioning parameters, such as shock intensity, its predictability, and inter-shock intervals, can also play crucial roles. Moreover, different

fear measures like freezing behavior, fear-potentiated startle, and inhibitory avoidance might manifest differently following varying conditioning protocols, adding another layer of complexity. A comprehensive understanding of fear memory strength will benefit from further studies scrutinizing these parameters and memory attributes. In addition, a growing body of evidence underscores the differences between males and females concerning fear memories [75]. Given that our study was conducted only with male rats, future studies exploring sex differences will be instrumental in providing a more complete account of the network-level mechanisms underlying fear memory strength.

In summary, this study investigated the behavioral and neural differences during the recall of memories with varying levels of aversiveness. In contrast to memories formed with a 2-shock fear conditioning protocol, 10 shocks generate maladaptive memories with intense and generalized fear responses, resistance to extinction, and an inability to flexibly change through reconsolidation. The recall of these memories resulted in changes in brain activation across some, but not all, regions where c-fos was measured. Graph-based network analysis uncovered that moderate and flexible fear memory expression involves an efficient integrated activation of particular brain regions, which is absent in strong fear memories. These results provide a deeper understanding of fear memory by showing that functional connectivity during recall varies greatly depending on the level of aversiveness of the memory. It supports the notion that not only local synaptic mechanisms but also broader functional changes play a role in shaping fear memory strength. Moreover, these findings highlight the importance of studying the neural mechanisms involved with fear memory strength, as they may provide insight into the development of maladaptive memories and potential interventions for their treatment.

Acknowledgments

We are grateful to Karine Gamache for technical support and Karine Gamache, Matteo Bernabo, and Isabelle Groves for their insights during the writing of the manuscript. This work was supported by Natural Sciences and Engineering Research Council of Canada (203523) and Canadian Institutes of Health Research (238757).

Conflict of Interest

The authors declare no competing interests or potential conflicts of interest.

REFERENCES

1. Flores Á, Fullana MÀ, Soriano-Mas C, Andero R. Lost in translation: how to upgrade fear memory research. Mol Psychiatry. 2018;23:2122–2132.
2. Fanselow MS. The role of learning in threat imminence and defensive behaviors. Current Opinion in Behavioral Sciences. 2018;24:44–49.
3. Homan P, Levy I, Feltham E, Gordon C, Hu J, Li J, et al. Neural computations of threat in the aftermath of combat trauma. Nat Neurosci. 2019;22:470–476.
4. Kredlow AM, Fenster RJ, Laurent ES, Ressler KJ, Phelps EA. Prefrontal cortex, amygdala, and threat processing: implications for PTSD. Neuropsychopharmacology. 2022;47:247–259.
5. Arellano Pérez AD, Popik B, de Oliveira Alvares L. Rewarding information presented during reactivation attenuates fear memory: Methylphenidate and fear memory updating. Neuropharmacology. 2020;171:108107.
6. Forcato C, Rodríguez MLC, Pedreira ME, Maldonado H. Reconsolidation in humans opens up declarative memory to the entrance of new information. Neurobiology of Learning and Memory. 2010;93:77–84.
7. Haubrich J, Crestani AP, Cassini LF, Santana F, Sierra RO, Alvares LDO, et al. Reconsolidation Allows Fear Memory to Be Updated to a Less Aversive Level through the Incorporation of Appetitive Information. Neuropsychopharmacology: Official Publication of the American College of Neuropsychopharmacology. 2014:1–12.
8. Monfils M-HH, Cowansage KK, Klann E, LeDoux JE. Extinction-reconsolidation boundaries: key to persistent attenuation of fear memories. Science. 2009;324:951–955.
9. Haubrich J, Bernabo M, Baker AG, Nader K. Impairments to Consolidation, Reconsolidation, and Long-Term Memory Maintenance Lead to Memory Erasure. Annual Review of Neuroscience. 2020;43.
10. Haubrich J, Machado A, Boos FZ, Crestani AP, Sierra RO, Alvares LDO, et al. Enhancement of extinction memory by pharmacological and behavioral interventions targeted to its reactivation. Scientific Reports. 2017;7.
11. Nader K, Schafe GE, Le Doux JE. Fear memories require protein synthesis in the amygdala for reconsolidation after retrieval. Nature. 2000;406:722–726.
12. Pigeon S, Lonergan M, Rotondo O, Pitman RK, Brunet A. Impairing memory reconsolidation with propranolol in healthy and clinical samples: a meta-analysis. J Psychiatry Neurosci. 2022;47:E109–E122.
13. Phelps EA, Hofmann SG. Memory editing from science fiction to clinical practice. Nature. 2019. 2019. https://doi.org/10.1038/s41586-019-1433-7.
14. Baldi E, Lorenzini CA, Bucherelli C. Footshock intensity and generalization in contextual and auditory-cued fear conditioning in the rat. Neurobiology of Learning and Memory. 2004;81:162–166.
15. Corchs F, Schiller D. Threat-related disorders as persistent motivational states of defense. Current Opinion in Behavioral Sciences. 2019;26:62–68.
16. Morey RA, Dunsmoor JE, Haswell CC, Brown VM, Vora A, Weiner J, et al. Fear learning circuitry is biased toward generalization of fear associations in posttraumatic stress disorder. Translational Psychiatry. 2015;5:e700.
17. Sangha S, Diehl MM, Bergstrom HC, Drew MR. Know Safety, No Fear. Neurosci Biobehav Rev. 2020;108:218–230.
18. Haubrich J, Nader K. Memory Reconsolidation. Current Topics in Behavioral Neurosciences, Springer Berlin Heidelberg; 2016. p. 1–26.

19. Holehonnur R, Phensy AJ, Kim LJ, Milivojevic M, Vuong D, Daison DK, et al. Increasing the GluN2A/GluN2B Ratio in Neurons of the Mouse Basal and Lateral Amygdala Inhibits the Modification of an Existing Fear Memory Trace. Journal of Neuroscience. 2016;36:9490–9504.
20. Kindt M. The surprising subtleties of changing fear memory: a challenge for translational science. Philosophical Transactions of the Royal Society B: Biological Sciences. 2018;373:20170033.
21. Wang S-H, de Oliveira Alvares L, Nader K. Cellular and systems mechanisms of memory strength as a constraint on auditory fear reconsolidation. Nature Neuroscience. 2009;12:905–912.
22. Sears RM, Schiff HC, LeDoux JE. Chapter Ten - Molecular Mechanisms of Threat Learning in the Lateral Nucleus of the Amygdala. In: Khan ZU, Muly EC, editors. Progress in Molecular Biology and Translational Science, vol. 122, Academic Press; 2014. p. 263–304.
23. Zhang W-H, Zhang J-Y, Holmes A, Pan B-X. Amygdala Circuit Substrates for Stress Adaptation and Adversity. Biological Psychiatry. 2021;89:847–856.
24. Conoscenti MA, Smith NJ, Fanselow MS. Dissociable consequences of moderate and high volume stress are mediated by the differential energetic demands of stress. PLOS ONE. 2022;17:e0273803.
25. Haubrich J, Bernabo M, Nader K. Noradrenergic projections from the locus coeruleus to the amygdala constrain fear memory reconsolidation. ELife. 2020;9:e57010.
26. Frankland PW, Josselyn SA, Köhler S. The neurobiological foundation of memory retrieval. Nat Neurosci. 2019;22:1576–1585.
27. Suzuki A, Josselyn S a, Frankland PW, Masushige S, Silva AJ, Kida S. Memory reconsolidation and extinction have distinct temporal and biochemical signatures. The Journal of Neuroscience : The Official Journal of the Society for Neuroscience. 2004;24:4787–4795.
28. Topolnik L, Tamboli S. The role of inhibitory circuits in hippocampal memory processing. Nat Rev Neurosci. 2022;23:476–492.
29. Barchiesi R, Chanthongdee K, Petrella M, Xu L, Söderholm S, Domi E, et al. An epigenetic mechanism for over-consolidation of fear memories. Mol Psychiatry. 2022;27:4893–4904.
30. de Oliveira Alvares L, Do-Monte FH. Understanding the dynamic and destiny of memories. Neuroscience & Biobehavioral Reviews. 2021;125:592–607.
31. Levy I, Schiller D. Neural Computations of Threat. Trends in Cognitive Sciences. 2021;25:151–171.
32. Milton AL. Fear not: recent advances in understanding the neural basis of fear memories and implications for treatment development. F1000Res. 2019;8:F1000 Faculty Rev-1948.
33. Debiec J, Bush DE, LeDoux JE. Noradrenergic enhancement of reconsolidation in the amygdala impairs extinction of conditioned fear in rats--a possible mechanism for the persistence of traumatic memories in PTSD. Depress Anxiety. 2011;28:186–193.
34. Gazarini L, Stern CA, Piornedo RR, Takahashi RN, Bertoglio LJ. PTSD-like memory generated through enhanced noradrenergic activity is mitigated by a dual step pharmacological intervention targeting its reconsolidation. Int J Neuropsychopharmacol. 2014;18.
35. Ressler KerryJ, Berretta S, Bolshakov VY, Rosso IM, Meloni EG, Rauch SL, et al. Post-traumatic stress disorder: clinical and translational neuroscience from cells to circuits. Nat Rev Neurol. 2022;18:273–288.
36. Terstege DJ, Epp JR. Network Neuroscience Untethered: Brain-Wide Immediate Early Gene Expression for the Analysis of Functional Connectivity in Freely Behaving Animals. Biology. 2023;12:34.
37. Bassett DS, Zurn P, Gold JI. On the nature and use of models in network neuroscience. Nat Rev Neurosci. 2018;19:566–578.
38. Bullmore E, Sporns O. Complex brain networks: graph theoretical analysis of structural and functional systems. Nat Rev Neurosci. 2009;10:186–198.

39. Roland AV, Coelho CAO, Haun HL, Gianessi CA, Lopez MF, D'Ambrosio S, et al. Alcohol dependence modifies brain networks activated during withdrawal and reaccess: a c-fos-based analysis in mice. Biological Psychiatry. 2023. 1 February 2023. https://doi.org/10.1016/j.biopsych.2023.01.018.
40. Silva BA, Burns AM, Gräff J. A cFos activation map of remote fear memory attenuation. Psychopharmacology. 2019;236:369–381.
41. Takeuchi T, Tamura M, Tse D, Kajii Y, Fernández G, Morris RGM. Brain region networks for the assimilation of new associative memory into a schema. Mol Brain. 2022;15:24.
42. Vetere G, Kenney JW, Tran LM, Xia F, Steadman PE, Parkinson J, et al. Chemogenetic Interrogation of a Brain-wide Fear Memory Network in Mice. Neuron. 2017;94:363-374.e4.
43. Wheeler AL, Teixeira CM, Wang AH, Xiong X, Kovacevic N, Lerch JP, et al. Identification of a Functional Connectome for Long-Term Fear Memory in Mice. PLoS Computational Biology. 2013;9:e1002853.
44. Haubrich J, Crestani a P, Cassini LF, Santana F, Sierra RO, de Oliveira Alvares L, et al. Reconsolidation allows fear memory to be updated to a less aversive level through the incorporation of appetitive information. Neuropsychopharmacology: Official Publication of the American College of Neuropsychopharmacology. 2015;40:315–326.
45. Watts DJ, Strogatz SH. Collective dynamics of 'small-world' networks. Nature. 1998;393:440–442.
46. Barrat A, Barthélemy M, Pastor-Satorras R, Vespignani A. The architecture of complex weighted networks. Proc Natl Acad Sci U S A. 2004;101:3747–3752.
47. Newman MEJ. Finding community structure in networks using the eigenvectors of matrices. Phys Rev E. 2006;74:036104.
48. Bernabo M, Haubrich J, Gamache K, Nader K. Memory Destabilization and Reconsolidation Dynamically Regulate the PKMζ Maintenance Mechanism. J Neurosci. 2021;41:4880–4888.
49. Gründemann J, Bitterman Y, Lu T, Krabbe S, Grewe BF, Schnitzer MJ, et al. Amygdala ensembles encode behavioral states. Science. 2019;364:eaav8736.
50. Josselyn SA, Köhler S, Frankland PW. Finding the engram. Nature Reviews Neuroscience. 2015;16:521–534.
51. Maddox SA, Hartmann J, Ross RA, Ressler KJ. Deconstructing the Gestalt: Mechanisms of Fear, Threat, and Trauma Memory Encoding. Neuron. 2019;102:60–74.
52. Do-Monte FH, Quiñones-Laracuente K, Quirk GJ. A temporal shift in the circuits mediating retrieval of fear memory. Nature. 2015;519:460–463.
53. Padilla-Coreano N, Do-Monte FH, Quirk GJ. A time-dependent role of midline thalamic nuclei in the retrieval of fear memory. Neuropharmacology. 2012;62:457–463.
54. Bloodgood DW, Sugam JA, Holmes A, Kash TL. Fear extinction requires infralimbic cortex projections to the basolateral amygdala. Transl Psychiatry. 2018;8:1–11.
55. Do-Monte FH, Manzano-Nieves G, Quiñones-Laracuente K, Ramos-Medina L, Quirk GJ. Revisiting the Role of Infralimbic Cortex in Fear Extinction with Optogenetics. J Neurosci. 2015;35:3607–3615.
56. Todd TP, Fournier DI, Bucci DJ. Retrosplenial cortex and its role in cue-specific learning and memory. Neurosci Biobehav Rev. 2019;107:713–728.
57. Trask S, Ferrara NC, Jasnow AM, Kwapis JL. Contributions of the rodent cingulate-retrosplenial cortical axis to associative learning and memory: A proposed circuit for persistent memory maintenance. Neurosci Biobehav Rev. 2021;130:178–184.
58. Ramanathan KR, Jin J, Giustino TF, Payne MR, Maren S. Prefrontal projections to the thalamic nucleus reuniens mediate fear extinction. Nat Commun. 2018;9:4527.
59. Sierra RO, Pedraza LK, Zanona QK, Santana F, Boos FZ, Crestani AP, et al. Reconsolidation-induced rescue of a remote fear memory blocked by an early cortical inhibition: Involvement of the

anterior cingulate cortex and the mediation by the thalamic nucleus reuniens. Hippocampus. 2017;27:596–607.
60. Troyner F, Bicca MA, Bertoglio LJ. Nucleus reuniens of the thalamus controls fear memory intensity, specificity and long-term maintenance during consolidation. Hippocampus. 2018;28:602–616.
61. Guo N, Soden ME, Herber C, Kim MTW, Besnard A, Lin P, et al. Dentate granule cell recruitment of feedforward inhibition governs engram maintenance and remote memory generalization. Nature Medicine. 2018;24:438–449.
62. Haubrich J, Nader K. A molecular mechanism governing memory precision. Nature Medicine. 2018;24.
63. Pedraza LK, Sierra RO, Boos FZ, Haubrich J, Quillfeldt JA, de Oliveira Alvares L. The dynamic nature of systems consolidation: Stress during learning as a switch guiding the rate of the hippocampal dependency and memory quality. Hippocampus. 2016;26:362–371.
64. da Silva TR, Raymundi AM, Bertoglio LJ, Andreatini R, Stern CA. Role of prelimbic cortex PKC and PKMζ in fear memory reconsolidation and persistence following reactivation. Sci Rep. 2020;10:4076.
65. Dixsaut L, Gräff J. Brain-wide screen of prelimbic cortex inputs reveals a functional shift during early fear memory consolidation. Elife. 2022;11:e78542.
66. Fernandez-Leon JA, Engelke DS, Aquino-Miranda G, Goodson A, Rasheed MN, Do Monte FH. Neural correlates and determinants of approach-avoidance conflict in the prelimbic prefrontal cortex. Elife. 2021;10:e74950.
67. Finnie PSB, Gamache K, Protopoulos M, Sinclair E, Baker AG, Wang S-H, et al. Cortico-hippocampal Schemas Enable NMDAR-Independent Fear Conditioning in Rats. Curr Biol. 2018;28:2900-2909.e5.
68. Haubrich J, Cassini LF, Diehl F, Santana F, Fürstenau de Oliveira L, de Oliveira Alvares L, et al. Novel learning accelerates systems consolidation of a contextual fear memory. Hippocampus. 2016;26.
69. Ortiz S, Latsko MS, Fouty JL, Dutta S, Adkins JM, Jasnow AM. Anterior Cingulate Cortex and Ventral Hippocampal Inputs to the Basolateral Amygdala Selectively Control Generalized Fear. The Journal of Neuroscience: The Official Journal of the Society for Neuroscience. 2019;39:6526–6539.
70. Bouton ME, Maren S, McNally GP. Behavioral and neurobiological mechanisms of pavlovian and instrumental extinction learning. Physiological Reviews. 2021;101:611–681.
71. Haubrich J, Bernabo M, Nader K. Noradrenergic projections from the locus coeruleus to the amygdala constrain fear memory reconsolidation. ELife. 2020. 18 May 2020. https://doi.org/10.7554/eLife.57010.
72. Haubrich J, Crestani AP, Cassini LF, Santana F, Sierra RO, Alvares L de O, et al. Reconsolidation Allows Fear Memory to Be Updated to a Less Aversive Level through the Incorporation of Appetitive Information. Neuropsychopharmacology. 2015;40:315–326.
73. Poulos AM, Mehta N, Lu B, Amir D, Livingston B, Santarelli A, et al. Conditioning- and time-dependent increases in context fear and generalization. Learning and Memory. 2016;23:379–385.
74. Gazarini L, Stern CAJ, Bertoglio LJ. On making (and turning adaptive to) maladaptive aversive memories in laboratory rodents. Neuroscience & Biobehavioral Reviews. 2023;147:105101.
75. Fleischer AW, Frick KM. New perspectives on sex differences in learning and memory. Trends in Endocrinology & Metabolism. 2023. 25 July 2023. https://doi.org/10.1016/j.tem.2023.06.003.

FIGURE LEGENDS

Figure 1. Behavioral differences triggered by CFC using different numbers of foot shocks.

A) Animals were placed in a fear conditioning box for ten minutes and received either no foot shock (NS group), two shocks (2S group), or ten shocks (10S group). One day later they returned to the same context for 4 minutes (Test A), and on the following day were placed for 4 minutes in a new, distinct context (Test B). The next day, rats were placed for 10 minutes in an open field arena. During training, freezing behavior increased following shock presentations in both 2S and 10S groups (N = 6 / 8 per group). In both Test A and B (left), animals trained with 10 shocks displayed higher freezing levels than other groups, and animals that received no shock displayed the lowest freezing. To assess how animals from the 2S and 10S groups differed regarding fear generalization, an index was calculated (Freezing in Test 2 / Freezing in Test 1 + Test 2), revealing that 10S animals expressed higher generalization (center). In the open field test, there were no differences between groups across parameters of exploratory behavior (right).

B) Animals were submitted to the 2S and 10S training protocols and on the next day were re-exposed to the training context for 30 minutes to induce extinction learning. The next day, a 4 minutes test was performed to evaluate extinction retention. Throughout the extinction session, both groups exhibited a decrease in fear expression but 10S animals displayed significantly higher freezing. In the test session, 2S animals displayed extinction retention, with no increase in freezing in comparison to the last 5 minutes bin of the extinction session, whereas 10S animals displayed a return of fear to the levels of the first bin.

C) Animals were submitted to the 2S and 10S training protocols and the next day the fear memory was reactivated by re-exposing animals to the training context for 4 minutes. Immediately after the reactivation session, anisomycin or its vehicle was injected i.p. to block memory reconsolidation. The efficiency of the reconsolidation was assessed the next day in a test where animals were again exposed to the conditioned context for 4 minutes. In the 2S group, anisomycin treatment lead to a decrease in fear expression, whereas the same treatment was ineffective in the 10S group.

Plots show the mean ± s.e.m. N = 8 per group. *$p < 0.05$.

Figure 2. Retrieval-induced brain activation of neutral, mild, and strong fear memories.

A) Animals were submitted to the NS, 2S, or 10S training protocols. To trigger the recall of the resulting memory, one day after training rats returned to the same context for 4 minutes, and 90 minutes later, brains were extracted for c-fos immunohistochemistry. During the test, animals in the 10S displayed higher freezing levels than all others, and 2S animals froze more than NS animals.

B) Boundaries of the regions targeted for c-fos quantification. Twelve regions were analyzed: in the hippocampus, the dentate gyrus (DG) and the CA3 and CA1 subfields; the basolateral (BLA) and the central (CeA) nuclei of the amygdala; the retrosplenial (RSC), infralimbic (IL), prelimbic (PL), and cingulate cortices (Cg1 and Cg2); the reuniens (Re) and paraventricular (PV) nuclei of the thalamus.

C) In the BLA, CeA, and PV, both 2S and 10S displayed higher c-fos expression than NS. In the CeA and PV, both 10S also displayed higher c-fos expression than 2S. In the Re and RSC, only the 2S group showed higher c-fos counts than the NS. In the IL, c-fos expression was reduced in the 10S group in comparison to 2S.

Plots show the mean ± s.e.m. N = 8 per group. *$p < 0.05$.** $p < 0.01$. *** $p < 0.001$. **** $p < 0.0001$.

Figure 3. Altered functional connectivity during mild and strong fear memory recall.

A) Color-coded matrices showing the interregional correlation values in the NS, 2S, and 10S groups. The diagonals were zeroed.

B) Mean r values were higher in the 2S group than in the others.

C) The 2S group displayed higher mean r values than the other groups in all regions except in the HPC, where it did not differ from 10S.

Plots show the median ± CI. *$p < 0.05$.** $p < 0.01$. *** $p < 0.001$.

Figure 4. Analysis of functional brain networks engaged by the recall of mild and strong fear memories.

A) Unfiltered networks comprising nodes representing brain regions, and edges representing the intercorrelation value between each pair of regions. The edges' width scale with its weight (absolute r-value) and colors indicate the real r-value.

B) R values that were retained after thresholding (between dotted lines) and assigned as edges in the functional memory networks.

C) Left: Degree distribution in each group. Right: The mean degree was higher in the 2S group than in NS and 10S groups. * $p < 0.05$. ** $p < 0.01$

D) Left: Betweenness distribution in each group. Right: The mean betweenness was higher in the 2S than in NS and 10S. * $p < 0.05$.

E) Left: Nodal efficiency distribution in each group. Right: The global efficiency was higher in the 2S than in NS and 10S, and only in the 2S group it matched that of random networks with small-world configuration. * $p < 0.05$. # confidence interval for the difference between means > 95%.

D) Representation of the functional networks of the NS (left), 2S (center), and 10S (right) groups. The nodes represent brain regions and the edges represent the functional connections between them. The nodes' sizes are scaled according to their degree, and the edges are scaled according to their r value. Nodes detected as being part of the same cluster are highlighted with the same color.

Plots show the median ± CI.

Figure 1

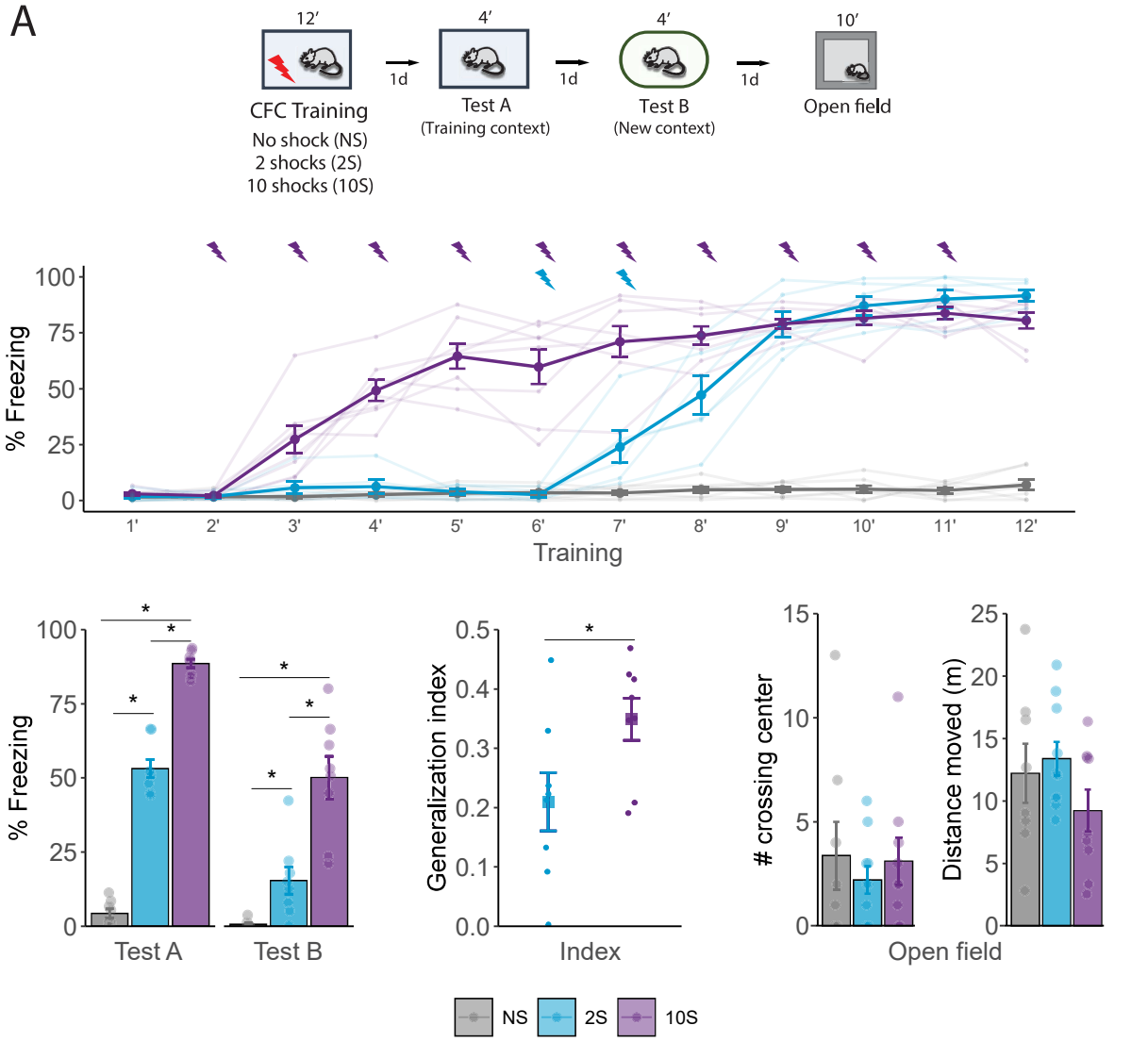
A
12′
4′
4′
10′
1d
1d
1d
CFC Training
No shock (NS)
2 shocks (2S)
10 shocks (10S)
Test A
(Training context)
Test B
(New context)
Open field
% Freezing
Training
Test A
Test B
Generalization index
Index
crossing center
Distance moved (m)
Open field
NS
2S
10S

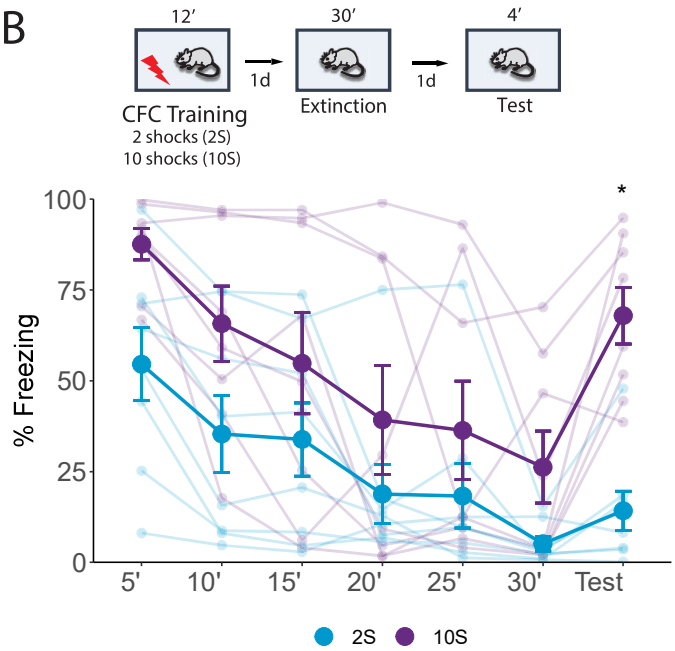
B
12′
30′
4′
1d
1d
CFC Training
2 shocks (2S)
10 shocks (10S)
Extinction
Test
% Freezing
5'
10'
15'
20'
25'
30'
Test
2S
10S

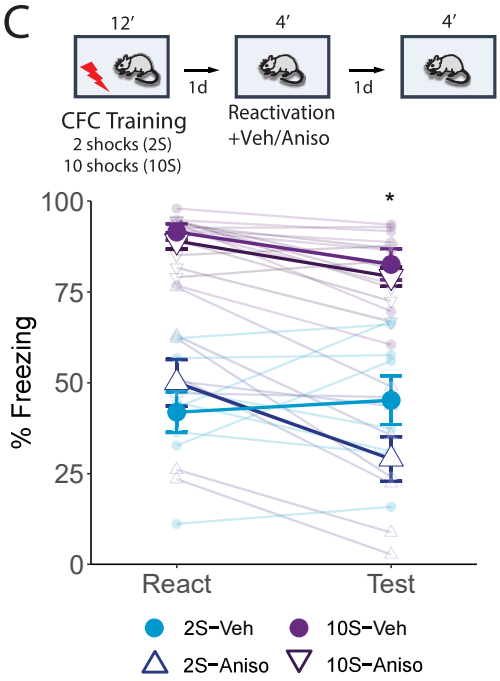
C
12′
4′
4′
1d
1d
CFC Training
2 shocks (2S)
10 shocks (10S)
Reactivation
+Veh/Aniso
% Freezing
React
Test
2S-Veh
10S-Veh
2S-Aniso
10S-Aniso

Figure 2

A

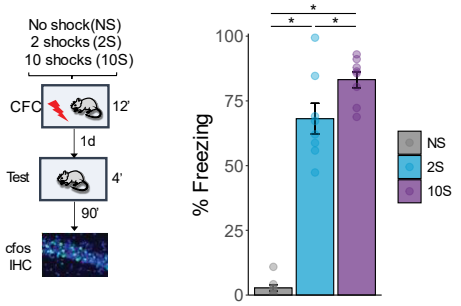
No shock(NS)
2 shocks (2S)
10 shocks (10S)
CFC
12'
1d
Test
4'
90'
cfos
IHC
% Freezing
100
75
50
25
0
*
*
*
NS
2S
10S

B

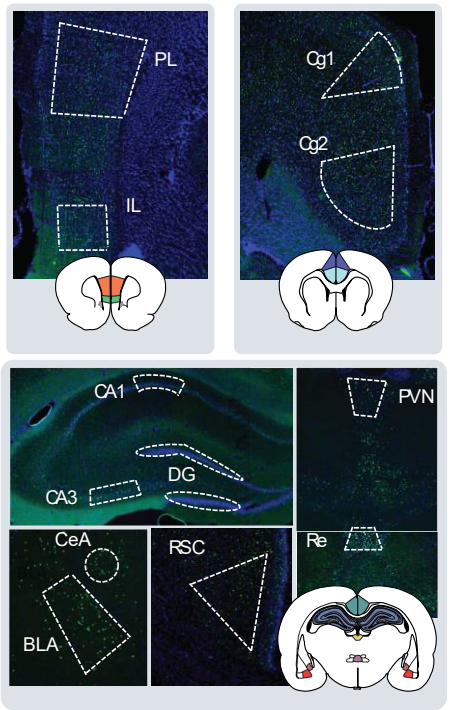
PL
IL
Cg1
Cg2
CA1
DG
CA3
PVN
CeA
BLA
RSC
Re

C

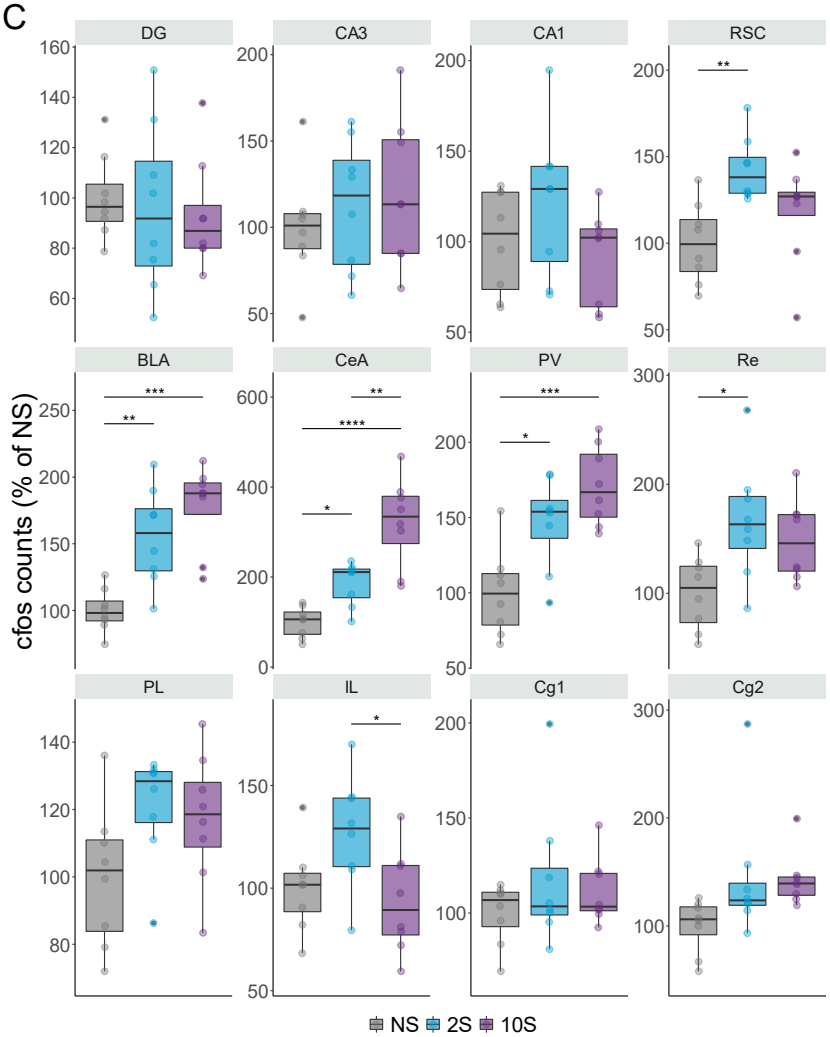
DG
CA3
CA1
RSC
BLA
CeA
PV
Re
PL
IL
Cg1
Cg2
cfos counts (% of NS)
NS
2S
10S

Figure 3

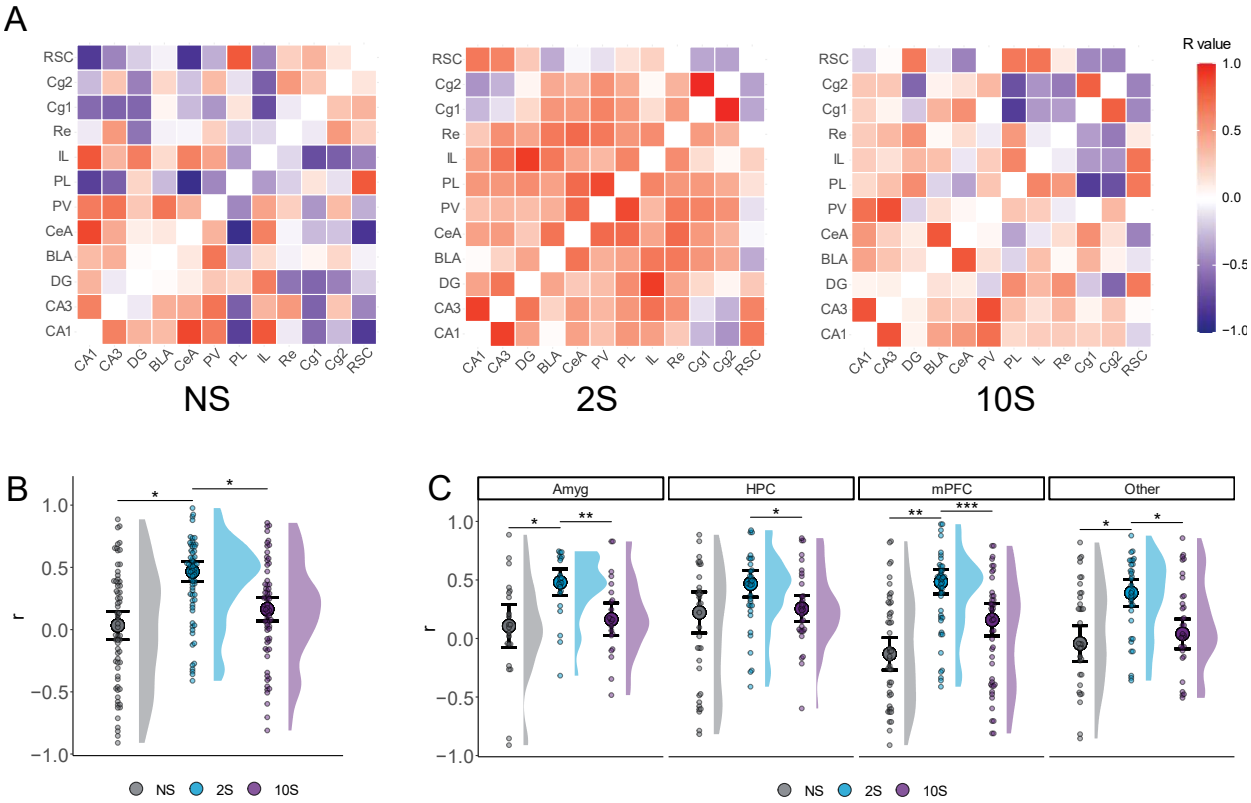
A
RSC
Cg2
Cg1
Re
IL
PL
PV
CeA
BLA
DG
CA3
CA1
NS
2S
10S
R value
1.0
0.5
0.0
−0.5
−1.0
B
r
NS
2S
10S
C
Amyg
HPC
mPFC
Other

Figure 4

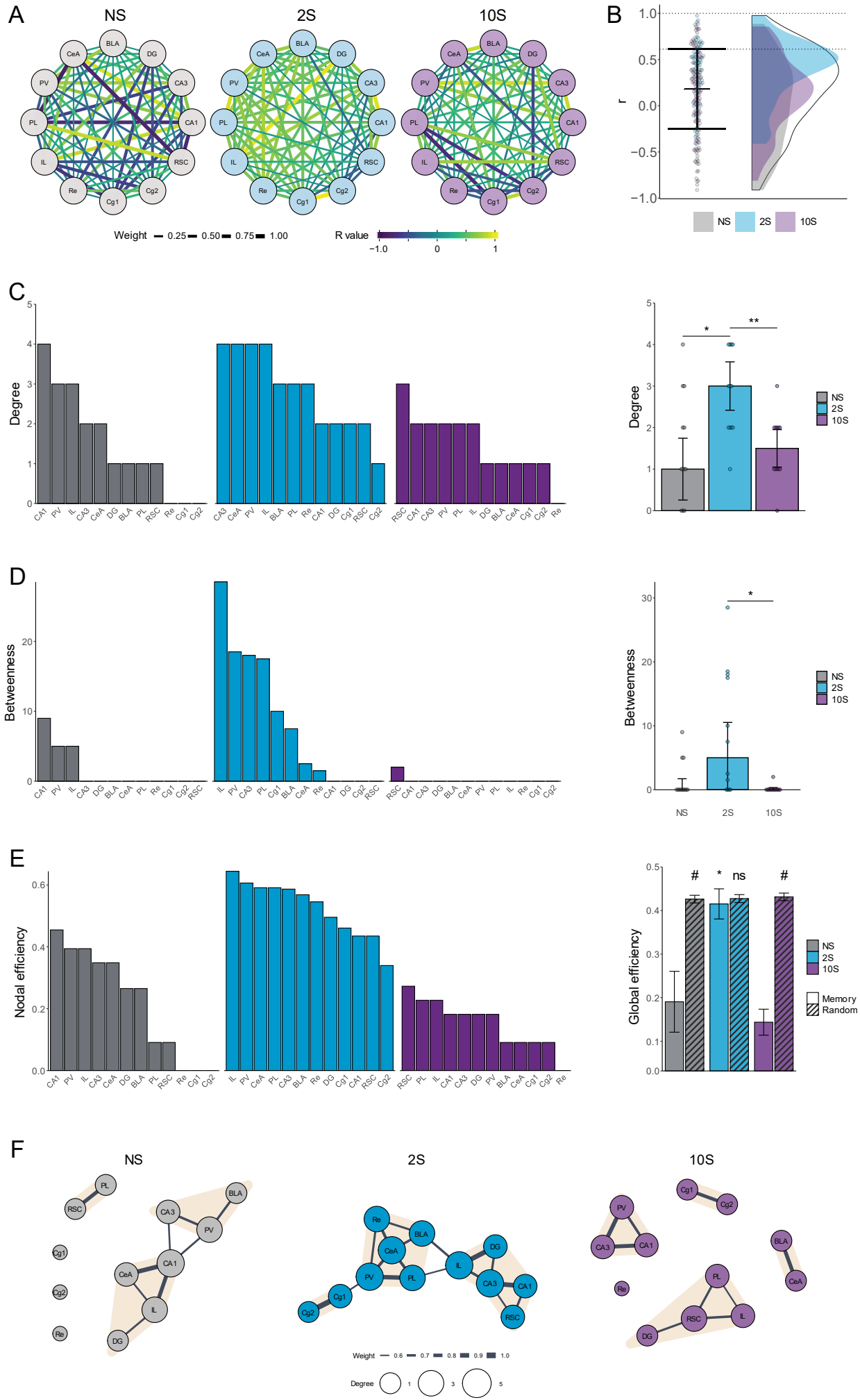
A
NS
2S
10S
BLA
DG
CA3
CA1
RSC
Cg2
Cg1
Re
IL
PL
PV
CeA
Weight 0.25 0.50 0.75 1.00
R value
−1.0
0
1
B
r
1.0
0.5
0.0
−0.5
−1.0
NS
2S
10S
C
Degree
*
**
D
Betweenness
*
E
Nodal efficiency
Global efficiency
#
*
ns
#
Memory
Random
F
Weight 0.6 0.7 0.8 0.9 1.0
Degree 1 3 5